JVI Journals.ASM.org

Functional Characterization of Residues Required for the Herpes Simplex Virus 1 E3 Ubiquitin Ligase ICP0 To Interact with the Cellular E2 Ubiquitin-Conjugating Enzyme UBE2D1 (UbcH5a)

Emilia Vanni, Derek Gatherer, Lily Tong, Roger D. Everett, and Chris Boutell

MRC—University of Glasgow Centre for Virus Research, Glasgow, Scotland, United Kingdom

The viral ubiquitin ligase ICP0 is required for efficient initiation of herpes simplex virus 1 (HSV-1) lytic infection and productive reactivation of viral genomes from latency. ICP0 has been shown to target a number of specific cellular proteins for proteasome-dependent degradation during lytic infection, including the promyelocytic leukemia protein (PML) and its small ubiquitin-like modified (SUMO) isoforms. We have shown previously that ICP0 can catalyze the formation of unanchored polyubiquitin chains and mediate the ubiquitination of specific substrate proteins *in vitro* in the presence of two E2 ubiquitin-conjugating enzymes, namely, UBE2D1 (UbcH5a) and UBE2E1 (UbcH6), in a RING finger-dependent manner. Using homology modeling in conjunction with site-directed mutagenesis, we identify specific residues required for the interaction between the RING finger domain of ICP0 and UBE2D1, and we report that point mutations at these residues compromise the ability of ICP0 to induce the colocalization of conjugated ubiquitin and the degradation of PML and its SUMO-modified isoforms. Furthermore, we show that RING finger mutants that are unable to interact with UBE2D1 fail not only to complement the plaque-forming defect of an ICP0-null mutant virus but also to mediate the derepression of quiescent HSV-1 genomes in cell culture. These data demonstrate that the ability of ICP0 to interact with cellular E2 ubiquitin-conjugating enzymes is fundamentally important for its biological functions during HSV-1 infection.

The herpes simplex virus 1 (HSV-1) immediate-early (IE) protein ICP0 is required for the efficient initiation of lytic infection (26, 33, 65, 71) and productive reactivation from latency (7, 47, 66, 67). Provision of exogenous ICP0 has been shown to complement the plaque formation efficiency (PFE) defect of an ICP0-null mutant virus (13, 26, 33) and to stimulate gene expression from quiescent viral genomes (33, 36, 37, 43, 62, 64). Importantly, both of these activities are dependent on the N-terminal RING finger domain of ICP0 (20, 21, 33, 43), a motif that belongs to a class of zinc-coordinating C_3HC_4 RING fingers (1, 25). During infection, the RING finger domain of ICP0 acts as an E3 ubiquitin ligase targeting specific cellular proteins for proteasome-dependent degradation (5). Substrates of ICP0 include proteins involved in DNA repair (46, 49, 61), centromere assembly (28, 51–53), and intrinsic antiviral resistance (3, 9, 29, 32, 34, 59). One of the most prominent substrates of ICP0 is the major nuclear domain 10 (ND10) constituent PML (promyelocytic leukemia protein) and its small ubiquitin-like modified (SUMO) isoforms, which have been linked with intrinsic antiviral immunity in response to HSV-1 infection (12, 32, 34). ICP0 also has some properties related to those of SUMO-targeted ubiquitin ligases (STUbLs), inducing the degradation of high-molecular-weight SUMO-conjugated proteins during infection in a RING finger-dependent manner (3, 29). *In vitro*, the RING finger domain of ICP0 catalyzes the formation of unanchored polyubiquitin chains in the presence of two E2 ubiquitin-conjugating enzymes, UBE2D1 (UbcH5a) and UBE2E1 (UbcH6) (5), and mediates the ubiquitination of various substrate proteins, including the tumor suppressor protein 53 (p53), ubiquitin-specific protease 7 (USP7), RNF8, and poly-SUMO-2 chains (2–4, 49). Exogenous expression of a catalytically inactive form of UBE2D1 inhibits ICP0-mediated degradation of PML (40), indicating that the interaction of ICP0 with UBE2D1 is functionally relevant.

Despite the observations that the RING finger domain of ICP0 has ubiquitin ligase activity in the presence of UBE2D1 and UBE2E1 and that both of these E2 enzymes colocalize with ICP0 foci in a RING finger-dependent manner (5), the residues required for these interactions have not been defined. Previous analysis has shown that viruses with mutations in the zinc-coordinating C_3HC_4 consensus residues have phenotypes similar to those of an ICP0-null mutant virus or a RING finger deletion virus (1, 21, 27, 37, 39, 50), suggesting that the integrity of the RING finger domain is crucial for the biological function of ICP0 during infection. Mutational analysis at specific polar residues within the α-helix of the RING domain (1) demonstrated that mutation of K144, W146, Q148, or N151 did not affect the E3 ubiquitin ligase activity of ICP0 *in vitro* (5). However, these mutations had differing effects on the ability of ICP0 to induce the formation of colocalizing conjugated ubiquitin (24) and to stimulate viral replication, with mutations at N151 and K144 resulting in substantial HSV-1 growth defects (19). These data indicate that mutation of specific residues within the RING finger of ICP0 can potentially inhibit its transactivation properties during infection while supporting a degree of E2 interaction sufficient to stimulate the formation of polyubiquitin chains *in vitro*. To date, no direct interaction between the RING finger domain of ICP0 and its cognate E2 ubiquitin-conjugating enzymes has been reported.

The purpose of this study was to map the interaction interface

Received 23 December 2011 **Accepted** 9 March 2012
Published ahead of print 21 March 2012
Address correspondence to Chris Boutell, chris.boutell@glasgow.ac.uk.

doi:10.1128/JVI.07210-11

between the RING finger of ICP0 and its known E2 ubiquitin-conjugating enzyme partners, in particular UBE2D1, and to investigate the importance of these interactions for the function of ICP0 during HSV-1 infection. The accuracy of modeling of the ICP0 RING-UBE2D1 interaction interface is limited by the lack of a resolved structure of ICP0. The closest available structure to that of the ICP0 RING domain is the nuclear magnetic resonance (NMR) structure of the RING finger of the equine herpesvirus type 1 (EHV-1) orthologue, EICP0 (1). Predictions of the ICP0 RING finger residues required for the interaction with UBE2D1 were carried out by sequence alignment and computational homology modeling based on previously published structural data for other RING finger E3 ubiquitin ligases that form stable complexes with their cognate E2 ubiquitin-conjugating enzymes, namely, Casitas B-lineage lymphoma proto-oncogene (c-Cbl)-UBE2L3 (UbcH7) (72) and breast cancer early-onset 1 (BRCA1)-UBE2D3 (UbcH5c) (6, 58).

In this study, site-directed mutagenesis was used to mutate specific ICP0 RING finger residues corresponding to those required for other RING-E2 interactions (6, 58). Using yeast two-hybrid (Y2H) analysis, we demonstrate that residues within loops 1 and 2 of the ICP0 RING are required for detectable interaction with both UBE2D1 and UBE2E1. Mutation of these residues impaired or abolished the E3 ubiquitin ligase activity of ICP0 *in vitro* and inhibited its ability to conjugate ubiquitin and induce the degradation of PML in cell culture. Furthermore, RING finger mutants that were unable to interact with either UBE2D1 or UBE2E1 also failed to complement the plaque formation defect of an ICP0-null mutant virus and to induce the derepression of quiescent HSV-1 genomes. Molecular modeling of the ICP0 RING finger domain demonstrated that these residues form a potential contact interface with UBE2D1. These findings provide detailed insight into the biological importance of the ability of ICP0 to interact with components of the host cell ubiquitin pathway during lytic infection and the reactivation of viral genomes from quiescence, two fundamentally important aspects of the life cycle and replication of HSV-1.

MATERIALS AND METHODS

Plasmids. Site-directed mutagenesis of sequences encoding ICP0 RING finger residues A117, V118, T120, D121, I140, M147, P154, L155, and L160 was conducted using a QuikChange II kit (Stratagene) on plasmid pGEX241, a bacterial expression vector containing exons 1 and 2 (encoding the RING finger domain) of ICP0 linked in frame with the C terminus of glutathione *S*-transferase (GST) (5). Complementary oligonucleotides used for site-directed mutagenesis were as follows (5′-to-3′ sequences): for A117T, CGACGTGTGCACCGTGTGCACG; for V118A, CGTGTGC GCCGCGTGCACGGATGAG; for T120P, GCGCCGTGTGCCCGGATG AGATCG; for D121V, GCCGTGTGCACGGTTGAGATCGCGCC; for I140N, CCGCTTCTGCAACCCGTGCATGAAAACC; for M147R, GAAA ACCTGGAGGCAATTGCGC; for P154T, GCAACACCTGCACGCTGT GCAACG; for L155P, CACCTGCCCGCCGTGCAACGCC; and for L160R, GCAACGCCAAGCGGGTGTACCTG. The ICP0 RING finger deletion mutant ICP0-FXE (with residues 106 to 149 deleted) and the double cysteine zinc-binding mutant ICP0-RF (C116G C156A) were transferred into pGEX241 as NcoI-to-SacII fragments from cDNA vectors (20, 50). The DR40 (with residues 129 and 130 deleted), W146A, Q148E, and N151D ICP0 RING finger domain mutants have been described previously (5, 60). The RING finger mutants were transferred from their pGEX241 derivatives as XhoI-to-KpnI fragments into the p111 vector (expressing ICP0 under the control of the genomic IE-1 promoter sequences [22]) and as NcoI-to-KpnI fragments into the pGAD-ICP0 vector (3), or as XhoI-to-NotI fragments from their respective pGAD-ICP0 plasmids into the lentiviral vector pΔCMVTetOcICP0 (33). NdeI-to-EcoRI fragments of the resulting plasmids were used to construct lentiviral vectors based on pLKO.ΔCMV.TetO.cICP0 (33), which expresses ICP0 in a tetracycline-inducible manner.

The pET28aUbcH5a and pET28aUbcH6 plasmids, expressing polyhistidine-tagged UBE2D1 (UbcH5a) and UBE2E1 (UbcH6), have been described elsewhere (4). The UBE2D1 cDNA was transferred from pET28aHisUbcH5a as an NcoI-to-EcoRI fragment into plasmid pGBKT7 (Clontech). The coding sequences for UBE2B, UBE2R1, UBE2E1, and UBE2L3 were PCR amplified from their respective cDNA sources and were transferred into pGBKT7 for yeast two-hybrid (Y2H) analysis. A derivative of pGBKT7 containing the USP7 cDNA has been described previously (3).

***In vitro* E3 ubiquitin ligase assays.** Polyhistidine-tagged UBE2D1 and UBE2E1, and wild-type (wt) GST-241 and its mutant derivatives, were purified from bacterial extracts using affinity chromatography, as described previously (5). The polyhistidine-tagged E1 ubiquitin-activating enzyme was purified from baculovirus-infected cell extracts, as described previously (5). All ubiquitination reactions were carried out in a reaction buffer containing 50 mM Tris (pH 7.5), 50 mM NaCl, and 5 mM ATP and were stopped by the addition of 3× sodium dodecyl sulfate (SDS) gel loading buffer containing 8 M urea. Samples were boiled for 10 min prior to Western blot analysis. Ubiquitination reaction mixtures for the observation of polyubiquitin chain formation were incubated for 45 min at 37°C in the presence of 2.5 μg wt ubiquitin (Sigma-Aldrich), 10 ng E1, 30 ng wt or mutant forms of GST-241, and titrated amounts of the E2 ubiquitin-conjugating enzymes (as highlighted in Fig. 3). Ubiquitination reactions analyzing ICP0 autoubiquitination were carried out in the presence of 2.5 μg methylated ubiquitin (Boston Biochem), and the reaction mixtures were incubated for 15 min at 37°C prior to termination.

Antibodies. *In vitro* polyubiquitin chain formation and ICP0 autoubiquitination were detected by Western blot analysis using mouse monoclonal antibody (MAb) P4D1 (dilution, 1:1,000; Santa Cruz Biotechnology) and anti-ICP0 rabbit polyclonal serum r95 (27), respectively. ICP0 expression and PML expression were detected in the inducible cell system by Western blot analysis using MAb 11060 (dilution, 1:10,000) (27) and rabbit polyclonal antibody A301 (dilution, 1:500; Bethyl Laboratories). Actin was detected using MAb AC-40 (dilution, 1:1,000; Sigma-Aldrich) and was used as a loading control. Horseradish peroxidase-conjugated anti-mouse IgG (A4416; dilution, 1:1,000) and anti-rabbit IgG (A4914; dilution, 1:20,000) (both from Sigma-Aldrich) were used as secondary antibodies. ICP0 expression was detected using rabbit polyclonal antibody r190 (dilution, 1:200) (31), and conjugated ubiquitin was detected using MAb FK2 (dilution, 1:1,000; International Bioscience, Inc.) in immunofluorescence assays, as described previously (24). Appropriate secondary antibodies, Alexa Fluor 488-conjugated anti-rabbit IgG(H+L) (dilution, 1:1,000; Molecular Probes A21206) and Alexa Fluor 647-conjugated anti-mouse IgG(H+L) (dilution, 1:1,000; Molecular Probes A31571) (both from Invitrogen), were used.

Cell lines. HEp-2 cells were maintained in Dulbecco's modified Eagle medium (DMEM) supplemented with 10% fetal bovine serum (FBS) and 1% penicillin-streptomycin. HEK-293T cells, maintained in DMEM with the same supplements, were used to produce lentivirus stocks for the generation of cell lines inducibly expressing ICP0, as described previously (33). HA-TetR cells, expressing the EGFPnlsTetR fusion protein under the control of a full human cytomegalovirus (HCMV) promoter, were maintained in Williams Medium E (WME) supplemented with 10% FBS Gold, 1% penicillin-streptomycin, 1% L-glutamine, 0.5 μM hydrocortisone, 5 μg/ml insulin, and G418 (0.5 mg/ml), as described previously (33).

Viruses. The mutant viruses used in the study were *dl*1403/CMV*lacZ* (an HSV-1 ICP0-null mutant virus containing a *lacZ* gene within the *tk* locus under the control of the HCMV IE promoter; a kind gift from Chris Preston) and *in*1374 (a multiply defective virus containing the *ts*K lesion

within ICP4, a deletion within the ICP0 open reading frame [ORF], and a mutation in the activation domain of VP16) (63).

Yeast-two hybrid assay. Interactions between wt or RING finger mutant forms of ICP0 fused to the *GAL4* DNA activation domain (AD) and cellular proteins fused to the *GAL4* DNA binding domain (BD) were tested by using the Matchmaker 3 system (Clontech) according to the manufacturer's instructions. Briefly, yeast strains AH109 and Y187 transformed with plasmids expressing the appropriate AD and BD fusion proteins, as indicated, were mated overnight and were plated onto a selective medium lacking leucine and tryptophan in order to confirm the presence of both expression vectors. Diploids were further plated onto a selective medium lacking leucine, tryptophan, and histidine and supplemented with 1 mM 3-amino-1,2,4-triazole (3-AT). The diploids were then incubated for 72 h prior to image capture.

Transfection and immunofluorescence analysis by confocal microscopy. Three hundred nanograms of p111 plasmid DNA expressing wt ICP0 or RING finger mutant derivatives was transfected into HEp-2 cells, which were seeded onto coverslips in 24-well dishes at 1×10^5 per well 1 day prior to transfection using Lipofectamine reagent (Invitrogen), according to the manufacturer's instructions. The cells were fixed at 6 h postoverlay, permeabilized, and stained for ICP0 and ubiquitin conjugates, as described previously (24). Samples were examined with a Zeiss LSM 510 confocal microscope using the 488-nm and 633-nm laser lines and were exported as tagged-image format files (TIFF) for presentation in Adobe Photoshop.

Generation of cell lines inducibly expressing ICP0. Lentivirus stocks were produced by transfecting approximately 50% confluent HEK-293T cell monolayers on 60-mm tissue culture dishes with 3 μg pLKO lentiviral plasmids containing coding sequences for wt and RING finger mutant forms of ICP0 and 3 μg of each helper plasmid (pCMV.DR8.91 and pVSV-G) using Lipofectamine reagent (Invitrogen), as described previously (33). Collected supernatants were used to serially transduce HA-TetR cells that were cultured in the presence of puromycin (initially 1 μg/ml for selection; then 0.5 μg/ml for maintenance), as described previously (33). ICP0 expression was induced with tetracycline (0.1 μg/ml) for 16 h.

Biological phenotype assays. The abilities of the ICP0 RING finger mutants to complement the plaque-forming defect of the ICP0-null mutant virus *dl*1403/CMV*lacZ* were tested in HA-TetR, wt HA-cICP0, and derivative inducible cell lines treated with tetracycline (0.1 μg/ml) at 16 h postinduction (33). Uninduced cells were analyzed in parallel as negative controls. Following infection for 1 h at 37°C, the cells were overlaid with fresh medium supplemented with 1% human serum and were incubated overnight at 37°C. The cells were washed twice in phosphate-buffered saline (PBS) and were fixed using 1% glutaraldehyde in PBS for 20 min, followed by two washes in PBS. The cells were incubated in 0.5 ml of 5-bromo-4-chloro-indolyl-galactopyranoside (X-gal) staining reagent (PBS supplemented with 5 mM potassium ferrocyanide, 2 mM magnesium chloride, 0.01% NP-40, and 2.4 mM X-gal in dimethyl sulfoxide [DMSO]) for 120 min at 37°C and were subsequently washed with water. β-Galactosidase-positive plaques were counted under an inverted light microscope (Olympus).

wt HA-cICP0 and derivative inducible cell lines were seeded into 24-well dishes at 1×10^5 cells per well and were incubated overnight at 37°C. Quiescence was established by infecting the cell monolayer with *in*1374 at a multiplicity of infection (MOI) of 5 PFU per cell for 1 h at the nonpermissive temperature of 38.5°C (33, 63). Infected cells were overlaid with fresh medium without added antibiotic selection and were incubated overnight at 38.5°C. Tetracycline (0.1 μg/ml) was used to induce ICP0 expression overnight at 38.5°C. The cells were subsequently stained for β-galactosidase expression to determine the level of derepression of the transcription of the *lacZ* marker gene in the *in*1374 genome. Derepression was quantified by capturing images in four random fields of view from three independently repeated experiments and counting cells positive for β-galactosidase expression, as described previously (33). The proportion of cells positive for β-galactosidase expression was expressed as a percentage of the number of induced wt HA-cICP0 cells positive for β-galactosidase.

Molecular modeling. Alignments of the E2 ubiquitin-conjugating enzyme sequences were carried out using ehmmalign (18) against the UQ_con (Pfam accession no. PF00179) hidden Markov model (HMM) from Pfam (38), and the best-substitution model was obtained using MEGA (44). This model was used to produce the best structural alignment of UBE2D1 (UbcH5a) with 1FBV chain C (UBE2L3/UbcH7) (72) using MOE-Align in MOE, version 2009 (Chemical Computing Group, Montreal, Quebec, Canada). ICP0 was aligned onto 1FBV chain A (c-Cbl) using MOE-Align (72). Multichain homology modeling for the ICP0-UBE2D1 complex was then carried out against 1FBV (72) using MOE, version 2009, without C-terminal and N-terminal outgap modeling, as follows. An initial proposed partial geometry was copied from the template chains in the solved structure of 1FBV by using all coordinates where residue identity was conserved. Otherwise, only backbone coordinates were used. Based on this initial partial geometry, Boltzmann-weighted randomized modeling (48) was employed with segment searching for regions that could not be mapped onto the initial partial geometry (35). One hundred models were constructed. On completion of segment addition, each model was energetically minimized in the AMBER-99 force field (70). The highest-scoring intermediate model was then determined by the generalized Born/volume integral (GB/VI) methodology (45). Ramachandran plots on the best model revealed only a small proportion of residues outside acceptable limits. Molecular surfaces were created using the method of Connolly (11), as applied within MOE.

RESULTS

Prediction of residues of the ICP0 RING finger domain that are required for its interaction with UBE2D1. Previous studies have shown that the RING finger domain of ICP0 has E3 ubiquitin ligase activity *in vitro* in the presence of two highly related E2 ubiquitin-conjugating enzymes: UBE2D1 (UbcH5a) and UBE2E1 (UbcH6) (2–5, 49). While there is evidence that UBE2D1 plays a role in ICP0 activity during HSV-1 infection (5, 40), the residues required for this interaction and its functional contribution to ICP0 activity have not been determined. Given the lack of structural information, prediction of ICP0 RING finger domain residues required for its interaction with UBE2D1 was carried out using homology modeling based on published E3-E2 complexes. An amino acid alignment of the RING finger domains of c-Cbl, BRCA1, ICP0, and its viral orthologue EICP0 (1) showed the highest degree of sequence homology at the zinc-coordinating residues and at residues within loop 2 (Fig. 1A). Previously mapped RING finger contacts in the c-Cbl-UBE2L3 (72) and BRCA1-UBE2D3 (6) complexes (residues marked with asterisks in Fig. 1A) indicated that the equivalent ICP0 RING residues are V118, T120, I140, P141, T145, W146, M147, L149, R150, T152, P154, L155, N157, A158, and L160 (Fig. 1A; not including zinc-coordinating residues). *In silico* homology modeling was performed by independent alignment of ICP0 and UBE2D1 onto the crystal structures of c-Cbl and UBE2L3 (1FBV) (72) using a combination of geometrical and conserved amino acid alignment. Of the 100 energetically minimized models generated, the highest-scoring model (Fig. 1B) was subsequently analyzed for amino acid conflicts and was determined to be within acceptable limits, as described in Materials and Methods. The final model was used to predict the ICP0 RING finger residues most likely to be major contacts with UBE2D1. Residues A117, V118, D121, W146, L149, and N157 were identified as likely interacting with UBE2D1 (Fig. 1B, orange spheres). Additional UBE2D1 contacts were predicted

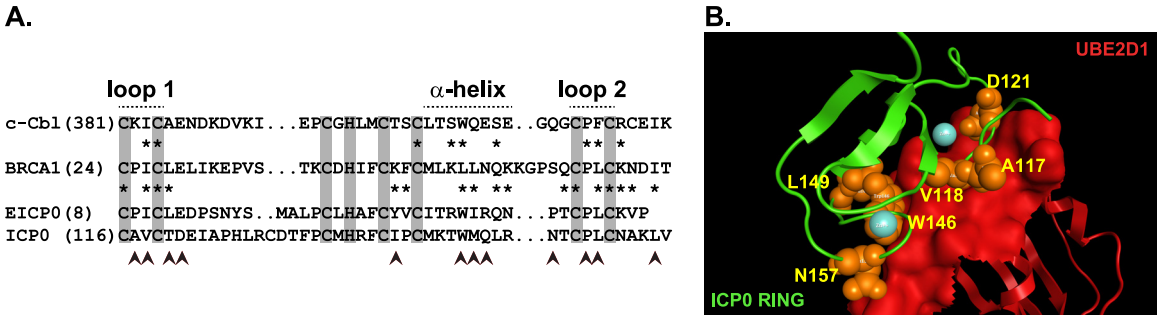

FIG 1 Prediction of the ICP0 RING finger residues required for interaction with UBE2D1. (A) Amino acid sequence alignment of the RING finger domains of c-Cbl (Swiss-Prot P22681), BRCA1 (P38398), EICP0 (P28990), and ICP0 (P08393). Zinc-coordinating residues are highlighted (gray vertical bars). Lines above the alignment indicate residues that form loop 1, loop 2, and the α-helix within the RING finger domain of ICP0. Asterisks indicate the residues of the RING finger domains of c-Cbl and BRCA1 required for interaction with their cognate E2 ubiquitin-conjugating enzymes (6, 72). The ICP0 RING finger residues chosen for mutagenesis in the current study, along with three previously characterized residues (W146, Q148, and N151) (5, 19, 24), are indicated by arrowheads. (B) Homology model of the ICP0 RING-UBE2D1 interaction interface based on the solved crystal structure of the c-Cbl-UBE2L3 (UbcH7) complex (1FBV) (72). Predicted contact residues between ICP0 (green) and UBE2D1 (red) are listed in Table 1. Contact residues within the ICP0 RING finger domain are shown as orange spheres and are annotated on the model. Bound zinc ions within the RING finger domain are presented as blue spheres.

to occur on the N-terminal side of the RING finger domain at positions G100, G101, R105, D107, and E112 (all predicted contact residues and bond types are summarized in Table 1).

Both the homology model and the sequence alignment suggested that contact points between ICP0 and UBE2D1 are located within the RING finger α-helix and loop regions (Fig. 1A and B), consistent with previous C_3HC_4 RING-E2 mapping studies (6, 14, 72). The prediction that residue W146 is involved in this interaction, however, contrasts with previous biological analyses, which demonstrated that mutation of this residue has no major effect on the E3 ubiquitin ligase activity of ICP0 *in vitro*, its ability to stimulate the formation of colocalizing conjugated ubiquitin, or the degradation of PML (5, 19, 24).

Based on this analysis, a panel of point mutants with changes at ICP0 residues A117, V118, T120, and D121 (loop 1), I140 and M147 (α-helix), and P154, L155, and L160 (loop 2) was generated. Mutation of the zinc-coordinating residues was avoided, because this would destabilize the structural integrity of the RING finger domain (20, 21, 37, 39, 50). Additionally, three previously characterized RING finger α-helix point mutants (the W146A, Q148E, and N151D mutants) were analyzed in parallel (5, 19, 24). Two negative controls were used throughout the study: ICP0-FXE, which carries a deletion of residues 106 to 149, containing the core RING finger domain (20, 21), and ICP0-RF, containing a double mutation of zinc-coordinating residues C116G and C156A (50). As an additional negative control, ICP0-DR40 (in which residues 129 and 130 are deleted) (60) was also analyzed *in vitro*. The phenotypes of these mutants in the assays carried out in this study are summarized in Table 2.

TABLE 1 Predicted contact points between the RING finger domain of ICP0 and UBE2D1 based on homology modeling[a]

ICP0 residue	UBE2D1 residue	Type of bond[b]
G100	D28	HB
G101	D28	HB
R105	Q14	HB
D107	K4	HB
D107	K4	ION
E112	K4	HB
E112	K8	HB
E112	K4	ION
E112	K8	ION
A117	R5	HB
V118	R5	HB
V118	F62	HYD
D121	L3	HB
D121	K4	HB
D121	L3	ION
W146	F62	HB
W146	F62	HYD
W146	W93	HYD
N157	Q92	HB
L149	F62	HYD

[a] See Fig. 1B.
[b] HB, hydrogen bond; ION, ionic bond; HYD, hydrophobic contact.

Mutation of specific residues in the ICP0 RING finger domain disrupts its interaction with UBE2D1 and UBE2E1. Since RING-E2 interactions are often transient, we used a Y2H assay to investigate the interaction of ICP0 with UBE2D1 and UBE2E1. wt and mutant forms of ICP0 were expressed as fusion proteins in which ICP0 was fused to the *GAL4* DNA activating domain (AD) and were tested for interaction with several E2 ubiquitin-conjugating enzymes expressed as fusion proteins in which the enzyme was fused to the *GAL4* DNA binding domain (BD). USP7 was used as a positive control for ICP0 interaction (30, 56, 57). wt ICP0, ICP0-FXE, and ICP0-RF all demonstrated strong interaction with USP7 in the presence of 3-AT (Fig. 2A), indicating that these proteins were efficiently expressed in yeast. wt ICP0 interacted with both UBE2D1 and UBE2E1 in a RING finger-dependent manner, as evidenced by the fact that both ICP0-FXE and ICP0-RF failed to interact with these enzymes (Fig. 2A). No interaction was observed between wt ICP0 and UBE2B, UBE2R1, or UBE2L3, indicating that the interactions of ICP0 with UBE2D1 and UBE2E1 were specific (Fig. 2A), consistent with the findings of *in vitro* biochemical assays (5). Screening of the panel of ICP0 RING mutants demonstrated that they all interacted with USP7, verifying ICP0 expression (Fig. 2B). The A117T, D121V, W146A, Q148E, and N151D ICP0 RING finger mutants all interacted with UBE2D1 and UBE2E1 (Fig. 2B). Mutation of residue V118, T120, I140, M147, P154, L155, or L160 reduced any interaction with both UBE2D1 and UBE2E1 below detectable levels (Fig. 2B).

TABLE 2 Summary of the phenotypes of the ICP0 RING finger mutants analyzed in this study

Phenotype[a]	wt	FXE[b]	RF	ICP0 RING finger mutant with the following mutation: A117T	V118A	T120P	D121V	I140N	W146A	M147R	Q148E	N151D	P154T	L155P	L160R
Y2H	+	−	−	+	−	−	+	−	+	−	+	+	−	−	−
UBE2D1															
Auto-ub	+	−	−	+	−	−	+	−	+	+/−	+	+/−	−	−	−
Poly-ub	+	−	−	+	+	+/−	+	+	+	+/−	+	+	+/−	−	+
UBE2E1															
Auto-ub	+	−	−	+	−	−	+/−	−	+	−	+	+/−	−	−	−
Poly-ub	+	−	−	+	+/−	−	+	+	+	−	+	+	−	−	−
FK2	+	−	−	+	+/−	−	+	+/−	+	+/−	+	+/−	+/−	−	−
PML degradation	+	−*	−	+	+	−	+	+/−	+	+/−	+	+/−	−	−	−
Complementation	+	−*	−	+	+	−	+	−	+	−	+	+/−	−	−	−
Derepression	+	−*	−	+	−	−	+	−	+	−	+/−	−	−	−	−

[a] The mutants' respective abilities to interact with E2 ubiquitin-conjugating enzymes (as determined by Y2H analysis [Fig. 2B]), catalyze the formation of polyubiquitin chains (poly-ub) and autoubiquitinate (auto-ub) in the presence of UBE2D1 or UBE2E1 stimulate the colocalization of conjugated ubiquitin (FK2), degrade PML, complement the PFE of *dl*1403/CMV*lacZ*, and derepress *lacZ* gene expression from quiescent *in*1374 viral genomes are indicated as follows: +, wt-like; −, ICP0-RF-like; +/−, intermediate.
[b] Asterisks indicate previously characterized phenotypes as described in reference 33.

Specific ICP0 RING finger point mutants have reduced E3 ubiquitin ligase activity *in vitro*. The RING finger domain of ICP0 catalyzes the formation of unanchored polyubiquitin chains and mediates autoubiquitination *in vitro* in the presence of UBE2D1 and UBE2E1 (5, 8). The panel of ICP0 RING finger mutants, expressed as GST fusion proteins in which the first 241 residues of ICP0 were fused with GST, was purified from bacterial extracts and was tested for *in vitro* ubiquitin ligase activity. Mutants GST-241-FXE, GST-241-RF, and GST-241-DR40 were used as negative controls (5, 39). Ubiquitin conjugation reactions were carried out in the presence of titrated amounts of purified UBE2D1 or UBE2E1 in order to observe potential differences in relative activities.

wt GST-241 and the W146A, Q148E, and N151D positive-control mutants all induced the formation of unanchored polyubiquitin chains in the presence of both UBE2D1 and UBE2E1, whereas no activity was detected for the negative controls GST-241-FXE, -RF, and -DR40 (Fig. 3A and B), consistent with previous studies (5, 39). Mutations at residues A117, V118, D121, and I140 did not affect polyubiquitin chain formation in the presence of either E2 enzyme, although the V118A mutant had reduced activity in the presence of UBE2E1 (Fig. 3B). The M147R and P154T mutants showed reduced activity with UBE2D1 (Fig. 3A) and no activity in the presence of UBE2E1 (Fig. 3B). The T120P and L160R mutants had significantly reduced activity in polyubiquitin chain formation in the presence of UBE2D1 (Fig. 3A) and were both inactive in the presence of UBE2E1 (Fig. 3B). The L155P mutant was completely inactive (Fig. 3A and B).

In agreement with previous results (5), wt GST-241 and the W146A, Q148E, and N151D mutants ubiquitinated themselves in the presence of methylated ubiquitin and both UBE2D1 and UBE2E1, while the negative controls GST-241-FXE, -RF, and -DR40 were inactive (Fig. 3C and D) (5). Mutations at residues A117 and D121 did not affect autoubiquitination, whereas mutations at residues V118, T120, I140, M147, P154, L155, and L160 impaired or abolished this activity (Fig. 3C and D). The activity of wt GST-241 was lower in the presence of UBE2E1 than in the presence of UBE2D1 (Fig. 3A to D), even though the two enzymes were equally active in thioester ubiquitin intermediate assays (data not shown). These data indicate that mutations at residues

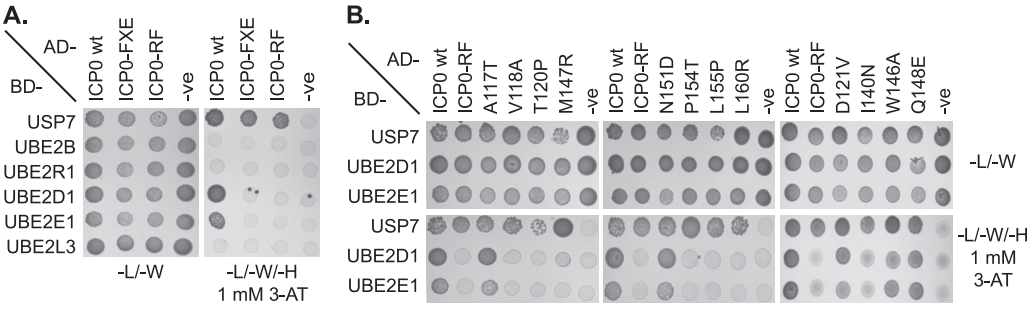

FIG 2 Specific ICP0 RING finger mutants fail to interact with E2 ubiquitin-conjugating enzymes. Full-length wt ICP0 and selected RING finger mutants (as shown) were expressed as fusion proteins in which ICP0 was linked to the *GAL4* DNA activating domain (AD) and were tested for interaction with USP7 and a panel of E2 ubiquitin-conjugating enzymes fused to the *GAL4* DNA binding domain (BD). Diploids were plated onto a medium lacking leucine and tryptophan (−L/−W) or a medium lacking leucine, tryptophan, and histidine (−L/−W/−H) and supplemented with 1 mM 3-AT to select for vector presence or protein interaction, respectively. (A) wt ICP0 interacts with specific E2 ubiquitin-conjugating enzymes in a RING finger-dependent manner in yeast. -ve, negative. (B) Specific point mutations within the RING finger domain of ICP0 abolish its ability to interact with UBE2D1 and UBE2E1.

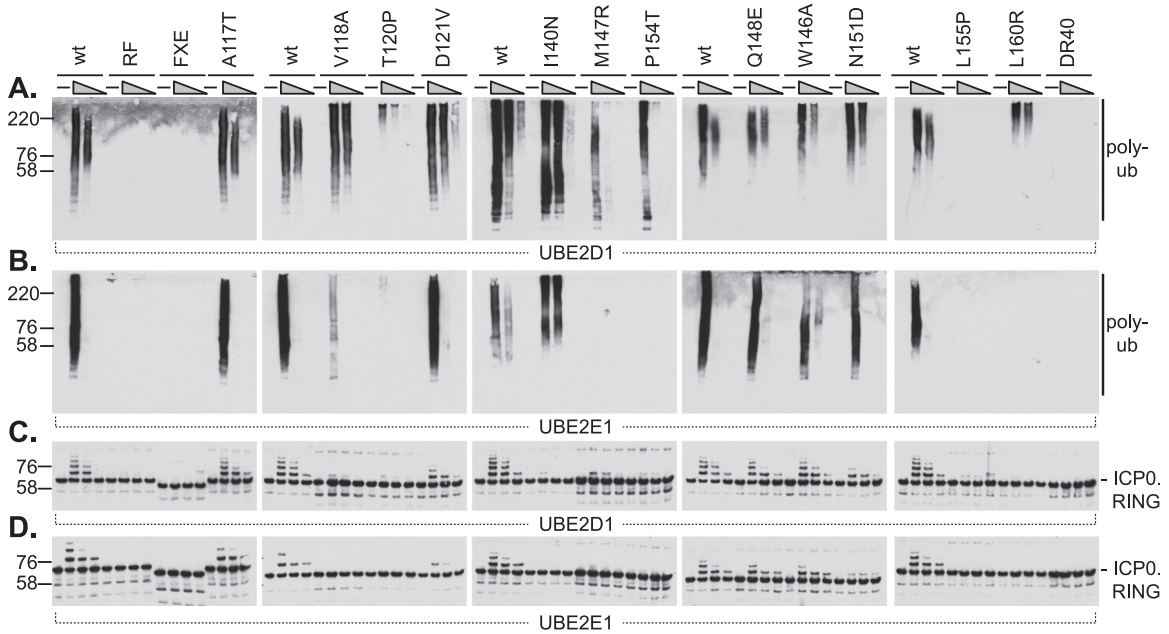

FIG 3 Specific ICP0 RING finger mutants have reduced E3 ubiquitin ligase activity *in vitro* in the presence of UBE2D1 and UBE2E1. wt and mutant ICP0 RING finger domains (amino acids 1 to 241) were purified from bacterial extracts as GST fusion proteins and were analyzed for their abilities to catalyze the formation of unanchored polyubiquitin (poly-ub) chains (A and B) or to undergo autoubiquitination (C and D) in the presence of titrated amounts (40, 20, or 8 ng) of UBE2D1 or UBE2E1 (as indicated). Polyubiquitin chains and ICP0 conjugates were detected by Western blotting using mouse monoclonal antibody P4D1 and rabbit polyclonal antibody r95, respectively.

V118, T120, M147, P154, L155, and L160 have an inhibitory effect on the E3 ubiquitin ligase activity of ICP0 *in vitro* in the presence of UBE2D1 and UBE2E1.

Specific ICP0 RING finger mutants fail to stimulate the formation of colocalizing conjugated ubiquitin in transfected cells. The ability of ICP0 to induce the disruption of ND10 and the degradation of PML correlates well with its ability to stimulate the RING finger-dependent formation of colocalizing conjugated ubiquitin in infected or transfected cells (24). Previous analysis has shown that the K144E and N151D RING mutants were inactive in this assay, whereas mutation of Q148 had no effect (24). However, both the K144E and N151D mutants retained E3 ubiquitin ligase activity *in vitro* (Fig. 3) (5). The reason for this difference between *in vitro* and cell culture assays is not clear but may reflect assay sensitivity or structural changes within the α-helix of the RING finger domain affecting E2 specificity. In order to validate our observations on the abilities of the RING finger mutants to interact with E2 enzymes (Fig. 2B) and their E3 ligase activities *in vitro* (Fig. 3A to D), we analyzed the formation of colocalizing conjugated ubiquitin in cells transfected with plasmids expressing full-length wt or RING finger mutant ICP0 proteins. We found that some mutants, for example, the A117T mutant, were active at wt levels in this assay, whereas others, including the T120P mutant, were inactive (Fig. 4A). The proportion of ICP0 foci that were positive for conjugated ubiquitin and the intensity of the signal differed between cells. Quantitative analysis was performed by counting the proportion of ICP0 foci that were ubiquitin positive. On this basis, the A117T, D121V, W146A, and Q148E mutants had wt activity in this assay, whereas the T120P, P154T, L155P, and L160R mutants had reduced activity, at levels similar to those of the negative controls ICP0-FXE and ICP0-RF (Fig. 4B). The V118A, I140N, and M147R mutants had intermediate activity, consistent with their reduced biochemical activity *in vitro* (Fig. 3). Consistent with previously published data (5, 24), the N151D mutant exhibited significantly reduced levels of conjugated ubiquitin colocalization (Fig. 4B), despite retaining wt biochemical activity *in vitro* (Fig. 3).

Characterization of the biological properties of the ICP0 RING finger mutants in cell culture. We recently described an inducible cell line system in which wt ICP0 can be expressed at physiological levels that fully complement the plaque formation defect of ICP0-null mutant HSV-1 and efficiently induce the derepression of quiescent viral genomes (33). This system allows comparison of the biological phenotypes of wt and RING finger mutant forms of ICP0 without the need to isolate recombinant viruses and their revertants. Lentiviral vectors were used to generate inducible cell lines expressing wt and RING finger mutant ICP0 proteins, as described previously (33). ICP0 was detected in these cell lines only following tetracycline induction (Fig. 5B) and was expressed in more than 90% of cells in each case (data not shown). Levels of PML were similar in all uninduced cell lines (Fig. 5A), while induction of wt ICP0, but not ICP0-RF, induced the degradation of PML (Fig. 5B). PML degradation was also observed in cells expressing the A117T, V118A, D121V, and I140N RING finger mutants, and in the W146A and Q148E positive-control mutants (19) (Fig. 5B). In contrast, PML remained relatively stable in cells expressing the T120P, M147R, N151D, P154T, L155P, and L160R mutants, indicating that mutation of these residues affects the ability of ICP0 to induce the efficient degradation of PML and its SUMO-modified isoforms. We note that this assay reflects the total abundance of PML following overnight induction of ICP0 and does not take into account any potential differences in the relative turnover rates between PML synthesis and ICP0-mediated degradation.

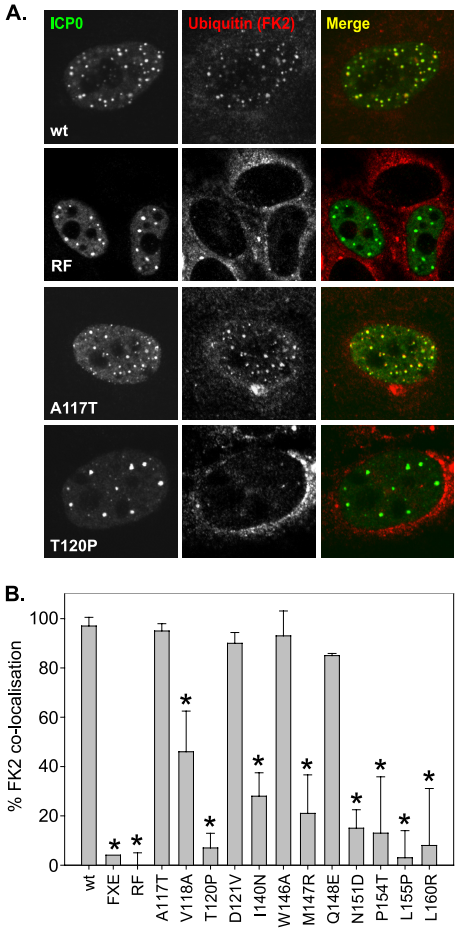

FIG 4 Specific ICP0 RING finger mutants fail to stimulate the colocalization of conjugated ubiquitin within transfected HEp-2 cells. (A) HEp-2 cells seeded onto coverslips were transfected with plasmids expressing full-length genomic wt ICP0 or RING finger mutants and were fixed at 6 h posttransfection. The cells were permeabilized and were stained for ICP0 and conjugated ubiquitin using the rabbit anti-ICP0 polyclonal antibody r190 and anti-conjugated ubiquitin MAb FK2, respectively. (B) Histogram depicting the percentages of ICP0 foci containing conjugated ubiquitin. ICP0 foci (totaling 100 foci over three independent experiments) were scored for the formation of colocalizing conjugated ubiquitin. The data for each mutant were analyzed in comparison to those for wt ICP0 by using the Mann-Whitney U test. Asterisks indicate statistically significant differences ($P < 0.02$).

Identification of RING finger mutants that fail to complement the plaque formation defect of ICP0-null mutant HSV-1. The requirement for ICP0 during HSV-1 replication is dependent on both multiplicity and cell type (26, 33, 71). The plaque-forming defect of ICP0-null mutant HSV-1 in HepRG cells is approximately 400-fold in comparison with the level of plaque formation in U2OS cells (26), in which ICP0 is not required for lytic replication (71). This defect is fully complemented in a RING finger-dependent manner in cells induced to express wt ICP0 (33). Therefore, we used this system to compare the complementation activities of wt and RING mutant forms of ICP0.

In the absence of tetracycline, no complementation activity was observed in any of the transduced cell lines (Fig. 6, filled bars). As expected from previous work (19), wt levels of complementation activity were observed in cells induced to express the W146A or Q148E mutant (Fig. 6, shaded bars). No complementation activity was observed in the negative-control cell line ICP0-RF, consistent with previous observations (33, 37, 39, 50). The A117T, V118A, and D121V RING finger mutants complemented the plaque formation efficiency defect to wt levels, whereas the T120P, I140N, M147R, P154T, L155P, and L160R mutants had signifi-

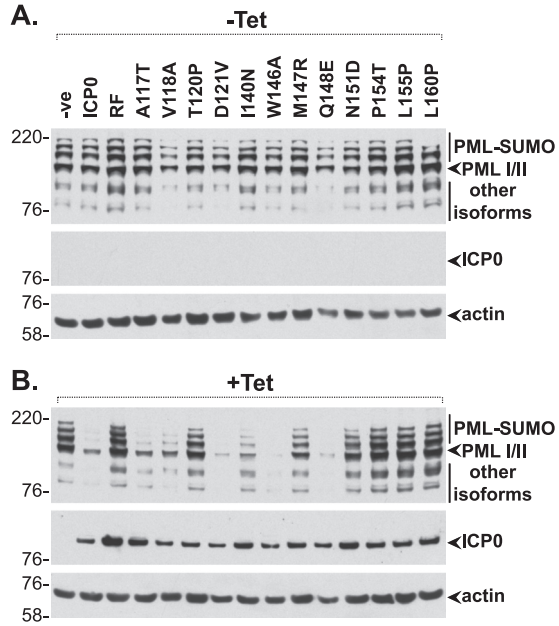

FIG 5 Specific ICP0 RING finger mutants fail to degrade PML in *trans*. Negative-control HA-TetR cells were transduced with lentiviruses expressing wt or RING finger mutant ICP0 proteins in a tetracycline-inducible manner. Cells were either left uninduced (−Tet) (A) or induced with tetracycline at 0.1 μg/ml (+Tet) for 16 h (B) prior to harvesting. Whole-cell lysates were analyzed by Western blotting for PML degradation and ICP0 expression using rabbit anti-PML (A301) and mouse anti-ICP0 (11060) antibodies, respectively. Actin was used as a loading control.

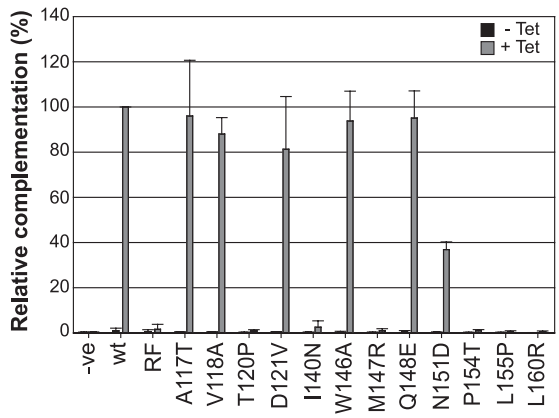

FIG 6 Specific ICP0 RING finger mutants fail to enhance the plaque formation efficiency of an ICP0-null mutant virus. wt and RING finger mutant ICP0 cell lines were assessed for complementation of an ICP0-null mutant virus (*dl*1403/CMV*lacZ*). Cells were either left uninduced (−Tet) (filled bars) or induced with 0.1 μg/ml tetracycline (+Tet) (shaded bars) for 16 h prior to infection. Twenty-four hours postinfection, cell monolayers were stained with X-gal; β-galactosidase-positive plaques were counted; and the number was expressed as a mean relative percentage of the complementation activity of wt ICP0. Error bars represent standard deviations from three independent experiments.

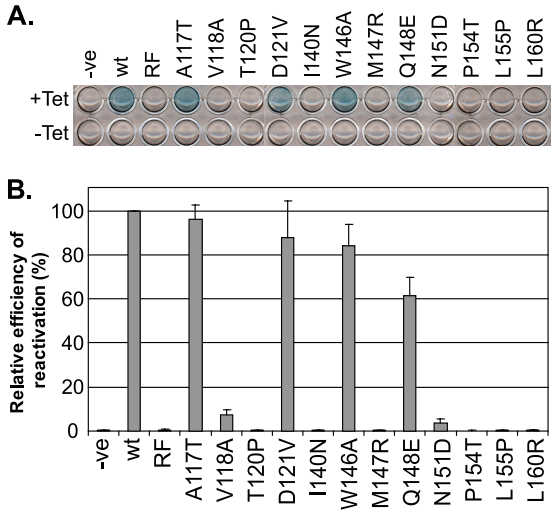

FIG 7 Specific ICP0 RING finger mutants fail to derepress gene expression from quiescent viral genomes. wt and RING finger mutant ICP0 cell lines were assessed for derepression of *lacZ* marker gene expression from quiescent *in*1374 viral genomes. Cells were infected with *in*1374 at an MOI of 5 PFU per cell at the nonpermissive temperature for 24 h in order to establish quiescence. The cells were then either left uninduced (−Tet) or induced with 0.1 μg/ml tetracycline (+Tet) for an additional 16 h at the nonpermissive temperature prior to X-gal staining. (A) Representative image showing β-galactosidase activity in cell monolayers induced to express wt or RING finger mutant ICP0 proteins, reflecting reactivated transcription from the *lacZ* reporter gene in the *in*1374 genome. (B) Quantification was carried out by counting β-galactosidase-positive cells and is expressed as a relative mean percentage of the reactivation of wt ICP0. Error bars represent standard deviations from three independent experiments.

cantly reduced levels of activity (Fig. 6). The N151D mutant showed an intermediate complementation phenotype, consistent with previously reported viral growth analysis of this mutant (19).

Identification of ICP0 RING finger mutants that fail to derepress quiescent HSV-1 gene expression. A critical function of ICP0 is to stimulate productive reactivation of HSV-1 from latency (7, 47, 66, 67). ICP0 is also able to induce gene expression from quiescent virus in cell culture (36, 37, 43, 62, 64). This activity also occurs in a RING finger-dependent manner in the inducible cell line system (33). Therefore, we analyzed the abilities of the ICP0 RING finger mutants to induce derepression of marker gene expression in cells quiescently infected with mutant *in*1374 (33, 63). The A117T, D121V, and W146A mutants had levels of activity similar to that of the wt protein in this assay, while the Q148E mutant was slightly less active than wt ICP0 (Fig. 7B). No derepression was detected in cells expressing the T120P, I140N, M147R, P154T, L155P, and L160R mutants, which had phenotypes equivalent to that of ICP0-RF (Fig. 7). Compared to that in negative controls, a low proportion of β-galactosidase-positive cells was observed following expression of the V118A and N151D mutants, but the levels were substantially reduced from that in wt ICP0 (Fig. 7). In the case of the T120P, P154T, L155P, and L160R mutants, these results parallel those of the complementation assay (Fig. 6B). However, it is surprising and striking that the V118A and N151D mutants had significant levels of complementation activity (Fig. 6B) yet were poorly active in the derepression assay. These data suggest that residues V118 and N151 may play a specific role in the ability of ICP0 to reactivate quiescent viral genomes from latency.

DISCUSSION

Viral E3 ubiquitin ligases counteract multiple aspects of antiviral immunity using a variety of mechanisms. For example, the Kasposi's sarcoma-associated herpesvirus (KSHV) protein K3 interacts with specific E2 ubiquitin-conjugating enzymes to induce both monoubiquitination and K63-linked polyubiquitination of major histocompatibility complex (MHC) class I molecules, resulting in their internalization and subsequent lysosomal degradation (17). This activity allows the virus to evade the cytotoxic T-cell response. During HSV-1 infection, ICP0 induces the RING finger-dependent degradation of a variety of cellular proteins implicated in multiple pathways, including intrinsic antiviral resistance (3, 32, 34), centromere assembly (28, 51–53), and DNA repair (49, 61). Importantly, the ability of ICP0 to induce the degradation of specific cellular substrates enhances viral replication efficiency and can be blocked by the addition of proteasome inhibitors (31, 32, 34). Therefore, the ability of ICP0 to stimulate viral infection is closely linked to its E3 ubiquitin ligase activity. While the RING finger domain of ICP0 has biochemical activity *in vitro* in the presence of UBE2D1 and UBE2E1 (2, 4, 5, 49), the contribution of these interactions to the biological functions of ICP0 was not fully elucidated previously. This study used site-directed mutagenesis to mutate predicted ICP0 RING-UBE2D1 interaction residues based on previous RING-E2 structural studies (6, 16, 72). The biochemical and biological properties of the mutants were characterized in comparison to those of wt ICP0 in order to determine the requirement for E2 ubiquitin-conjugating enzyme interaction. The data are summarized in Table 2.

Consistent with previous *in vitro* biochemistry and cellular localization studies (5), we demonstrated, by use of a Y2H assay, that ICP0 can specifically interact with the E2 enzymes UBE2D1 and UBE2E1 in a RING finger-dependent manner (Fig. 2). In contrast to previous reports (41, 42, 68), however, we could not detect an interaction between full-length ICP0 and UBE2R1 (cdc34) in our experimental system (Fig. 2). Our analysis is consistent with previous biochemical (5) and subsequent infection (23) studies, which demonstrated that the stability of UBE2R1 remains unaltered in the presence of ICP0. However, it is possible that ICP0 may interact with other E2 ubiquitin-conjugating enzymes, since other E3 ubiquitin ligases have been shown to interact with multiple E2 enzymes (6, 10, 15, 55, 69). We are currently addressing this possibility by screening a larger collection of E2 enzymes.

In contrast to our prediction and homology modeling (Fig. 1 and Table 1), mutation of ICP0 RING finger residues A117, D121, and W146 had no effect on ICP0 activity (Table 2), suggesting that these residues do not form major contact points with UBE2D1. Consistent with the previous characterization of residue W146 (5, 19, 24), our data show that while the conserved tryptophan residue may form an essential E2 interaction contact point in other RING E3 ligases (15, 72), it is not essential for the ICP0 RING-E2 interaction. Overall, we show that mutation of residue T120, I140, M147, P154, L155, or L160 within the RING domain of ICP0 disrupts interaction with UBE2D1 and UBE2E1, affects the E3 ubiquitin ligase activity of the RING domain *in vitro*, and significantly reduces its ability to stimulate the formation of colocalizing conjugated ubiquitin in transfected cells (Table 2). These data are consistent with the biological activities of these mutants, in that they fail not only to complement the plaque-forming defect of an ICP0-null mutant virus but also to induce the derepression of

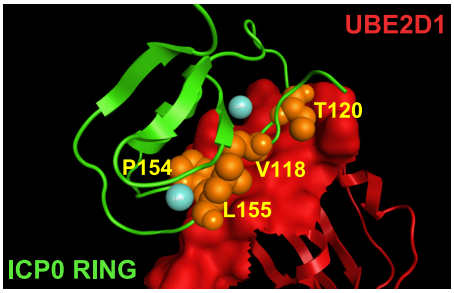

FIG 8 The ICP0 RING finger residues V118, T120, P154, and L155 align to the interaction interface with UBE2D1. Shown is a homology model of the ICP0 RING-UBE2D1 interaction interface (as described for Fig. 1B). ICP0 RING residues experimentally demonstrated to be required for UBE2D1 interaction are highlighted as orange spheres and are annotated. Bound zinc ions within the RING finger domain of ICP0 are depicted as blue spheres. The phenotypes of the ICP0 RING finger mutants characterized in this study are summarized in Table 2.

quiescent viral genomes in cell culture (Table 2). These data are also consistent with our computational modeling, which predicted that residues T120, P154, and L155 align to the interaction interface between the RING domain of ICP0 and UBE2D1 (Fig. 8, orange spheres).

There are some limitations to our assays that should be recognized. Although we did not observe interaction of the V118A, I140N, M147R, and P154T RING finger mutants with either UBE2D1 or UBE2E1 in the Y2H assay, these mutants retained some E3 ligase activity *in vitro* (Table 2). Therefore, mutations that weaken the RING-E2 interaction below the level of detection in the Y2H assay may allow sufficient E2 interaction for detectable biochemical activity and biological function. This could explain the behavior of the V118A mutant (Table 2). With the exception of V118A, however, there is a good correlation between the interaction of RING mutants with UBE2D1 in the Y2H assay and their overall biological phenotypes in complementation and derepression assays (Table 2). Surprisingly, although the N151D mutant interacted with and showed biochemical activity in the presence of UBE2D1 and UBE2E1, it did not induce efficient degradation of PML in the inducible cell line system (Fig. 5B and Table 2), consistent with previous analysis of this mutant during virus infection (5, 19). It is possible that ICP0 may use a combination of different E2 ubiquitin-conjugating enzymes for the ubiquitination of specific substrate proteins in a residue-dependent manner, or that mutation of N151 impacts the topology of the RING domain, which, in turn, affects substrate specificity and/or ubiquitination. The N151D mutant did, however, retain significant complementation activity, indicating that this mutant can at least partially overcome the repression of ICP0-null mutant HSV-1. It would therefore be of interest to study the effects of this mutant on other known mediators of intrinsic antiviral resistance (32, 54).

The most striking observation from our study was that while both the N151D and V118A mutations could increase ICP0-null mutant PFE, they were both unable to derepress gene expression from quiescent viral genomes (Fig. 7 and Table 2). These results suggest the intriguing hypothesis that ICP0 may have differential substrate specificities that govern complementation and reactivation from quiescence. Alternatively, reactivation from quiescence may involve ICP0 RING finger interactions with other E2 ubiquitin-conjugating enzymes that require specific residues within the RING domain, for example, V118 (Fig. 8). These differences may be important for understanding the mechanisms of viral reactivation from latency and the requirement of ICP0 and its E3 ubiquitin ligase activity for this process.

Our data indicate that residues V118, T120, P154, and L155 are likely to form a contact interface between the RING finger domain of ICP0 and its associated E2 ubiquitin-conjugating enzymes, including UBE2D1 and UBE2E1 (Fig. 8, orange spheres). Mutation of these residues significantly compromises the biological functions of the RING finger domain. Additional residues, such as the characterized L160 residue (Table 2), or the predicted residues P141, T145, L149, R150, T152, N157, and A158 (Fig. 1), which were not included in this study, could also form potential contacts, and these could be addressed in future studies. Overall, this study shows that the interaction of ICP0 with E2 ubiquitin-conjugating enzymes is essential for the ability of ICP0 to stimulate viral gene expression and reactivation from quiescence, two fundamental steps in the replication of HSV-1. Therefore, small-molecule inhibitors that block the ICP0-E2 interaction could have potential therapeutic value, especially since our data suggest that the ICP0-E2 interaction interface may be different from those of other cellular E3 ubiquitin ligases with regard to the contact residues within the α-helix of ICP0. However, a resolved crystal structure of the ICP0 RING finger domain is crucial for such studies and for any further detailed analysis of the ICP0 RING-E2 interaction interface.

ACKNOWLEDGMENTS

The work was conducted in the laboratory of Chris Boutell and was funded by the Medical Research Council.

We thank Chris Preston for the provision of numerous reagents and Delphine Cuchet-Lourenço and Mandy Glass for constructive comments during the preparation of the manuscript.

REFERENCES

1. **Barlow PN, Luisi B, Milner A, Elliott M, Everett R.** 1994. Structure of the C_3HC_4 domain by ^{1}H-nuclear magnetic resonance spectroscopy. A new structural class of zinc-finger. J. Mol. Biol. **237**:201–211.
2. **Boutell C, Canning M, Orr A, Everett RD.** 2005. Reciprocal activities between herpes simplex virus type 1 regulatory protein ICP0, a ubiquitin E3 ligase, and ubiquitin-specific protease USP7. J. Virol. **79**:12342–12354.
3. **Boutell C, et al.** 2011. A viral ubiquitin ligase has substrate preferential SUMO targeted ubiquitin ligase activity that counteracts intrinsic antiviral defence. PLoS Pathog. **7**:e1002245.
4. **Boutell C, Everett RD.** 2003. The herpes simplex virus type 1 (HSV-1) regulatory protein ICP0 interacts with and ubiquitinates p53. J. Biol. Chem. **278**:36596–36602.
5. **Boutell C, Sadis S, Everett RD.** 2002. Herpes simplex virus type 1 immediate-early protein ICP0 and its isolated RING finger domain act as ubiquitin E3 ligases in vitro. J. Virol. **76**:841–850.
6. **Brzovic PS, et al.** 2003. Binding and recognition in the assembly of an active BRCA1/BARD1 ubiquitin-ligase complex. Proc. Natl. Acad. Sci. U. S. A. **100**:5646–5651.
7. **Cai W, et al.** 1993. The herpes simplex virus type 1 regulatory protein ICP0 enhances virus replication during acute infection and reactivation from latency. J. Virol. **67**:7501–7512.
8. **Canning M, Boutell C, Parkinson J, Everett RD.** 2004. A RING finger ubiquitin ligase is protected from autocatalyzed ubiquitination and degradation by binding to ubiquitin-specific protease USP7. J. Biol. Chem. **279**:38160–38168.
9. **Chelbi-Alix MK, de Thé H.** 1999. Herpes virus induced proteasome-dependent degradation of the nuclear bodies-associated PML and Sp100 proteins. Oncogene **18**:935–941.
10. **Christensen DE, Brzovic PS, Klevit RE.** 2007. E2-BRCA1 RING interactions dictate synthesis of mono- or specific polyubiquitin chain linkages. Nat. Struct. Mol. Biol. **14**:941–948.

11. **Connolly ML.** 1983. Solvent-accessible surfaces of proteins and nucleic acids. Science **221**:709–713.
12. **Cuchet-Lourenço D, et al.** 2011. SUMO pathway dependent recruitment of cellular repressors to herpes simplex virus type 1 genomes. PLoS Pathog. **7**:e1002123.
13. **Davido DJ, von Zagorski WF, Lane WS, Schaffer PA.** 2005. Phosphorylation site mutations affect herpes simplex virus type 1 ICP0 function. J. Virol. **79**:1232–1243.
14. **Deshaies RJ, Joazeiro CA.** 2009. RING domain E3 ubiquitin ligases. Annu. Rev. Biochem. **78**:399–434.
15. **Dodd RB, et al.** 2004. Solution structure of the Kaposi's sarcoma-associated herpesvirus K3 N-terminal domain reveals a novel E2-binding C_4HC_3-type RING domain. J. Biol. Chem. **279**:53840–53847.
16. **Dominguez C, et al.** 2004. Structural model of the UbcH5B/CNOT4 complex revealed by combining NMR, mutagenesis, and docking approaches. Structure **12**:633–644.
17. **Duncan LM, et al.** 2006. Lysine-63-linked ubiquitination is required for endolysosomal degradation of class I molecules. EMBO J. **25**:1635–1645.
18. **Eddy SR.** 1998. Profile hidden Markov models. Bioinformatics **14**:755–763.
19. **Everett R, O'Hare P, O'Rourke D, Barlow P, Orr A.** 1995. Point mutations in the herpes simplex virus type 1 Vmw110 RING finger helix affect activation of gene expression, viral growth, and interaction with PML-containing nuclear structures. J. Virol. **69**:7339–7344.
20. **Everett RD.** 1988. Analysis of the functional domains of herpes simplex virus type 1 immediate-early polypeptide Vmw110. J. Mol. Biol. **202**:87–96.
21. **Everett RD.** 1989. Construction and characterization of herpes simplex virus type 1 mutants with defined lesions in immediate early gene 1. J. Gen. Virol. **70**(Pt 5):1185–1202.
22. **Everett RD.** 1987. A detailed mutational analysis of Vmw110, a *trans*-acting transcriptional activator encoded by herpes simplex virus type 1. EMBO J. **6**:2069–2076.
23. **Everett RD.** 2004. Herpes simplex virus type 1 regulatory protein ICP0 does not protect cyclins D1 and D3 from degradation during infection. J. Virol. **78**:9599–9604.
24. **Everett RD.** 2000. ICP0 induces the accumulation of colocalizing conjugated ubiquitin. J. Virol. **74**:9994–10005.
25. **Everett RD, et al.** 1993. A novel arrangement of zinc-binding residues and secondary structure in the C_3HC_4 motif of an alpha herpes virus protein family. J. Mol. Biol. **234**:1038–1047.
26. **Everett RD, Boutell C, Orr A.** 2004. Phenotype of a herpes simplex virus type 1 mutant that fails to express immediate-early regulatory protein ICP0. J. Virol. **78**:1763–1774.
27. **Everett RD, Cross A, Orr A.** 1993. A truncated form of herpes simplex virus type 1 immediate-early protein Vmw110 is expressed in a cell type dependent manner. Virology **197**:751–756.
28. **Everett RD, Earnshaw WC, Findlay J, Lomonte P.** 1999. Specific destruction of kinetochore protein CENP-C and disruption of cell division by herpes simplex virus immediate-early protein Vmw110. EMBO J. **18**:1526–1538.
29. **Everett RD, et al.** 1998. The disruption of ND10 during herpes simplex virus infection correlates with the Vmw110- and proteasome-dependent loss of several PML isoforms. J. Virol. **72**:6581–6591.
30. **Everett RD, et al.** 1997. A novel ubiquitin-specific protease is dynamically associated with the PML nuclear domain and binds to a herpesvirus regulatory protein. EMBO J. **16**:1519–1530.
31. **Everett RD, Orr A, Preston CM.** 1998. A viral activator of gene expression functions via the ubiquitin-proteasome pathway. EMBO J. **17**:7161–7169.
32. **Everett RD, Parada C, Gripon P, Sirma H, Orr A.** 2008. Replication of ICP0-null mutant herpes simplex virus type 1 is restricted by both PML and Sp100. J. Virol. **82**:2661–2672.
33. **Everett RD, Parsy ML, Orr A.** 2009. Analysis of the functions of herpes simplex virus type 1 regulatory protein ICP0 that are critical for lytic infection and derepression of quiescent viral genomes. J. Virol. **83**:4963–4977.
34. **Everett RD, et al.** 2006. PML contributes to a cellular mechanism of repression of herpes simplex virus type 1 infection that is inactivated by ICP0. J. Virol. **80**:7995–8005.
35. **Fechteler T, Dengler U, Schomburg D.** 1995. Prediction of protein three-dimensional structures in insertion and deletion regions: a procedure for searching data bases of representative protein fragments using geometric scoring criteria. J. Mol. Biol. **253**:114–131.
36. **Ferenczy MW, DeLuca NA.** 2011. Reversal of heterochromatic silencing of quiescent herpes simplex virus type 1 by ICP0. J. Virol. **85**:3424–3435.
37. **Ferenczy MW, Ranayhossaini DJ, Deluca NA.** 2011. Activities of ICP0 involved in the reversal of silencing of quiescent herpes simplex virus 1. J. Virol. **85**:4993–5002.
38. **Finn RD, et al.** 2010. The Pfam protein families database. Nucleic Acids Res. **38**:D211–D222.
39. **Grant K, Grant L, Tong L, Boutell C.** 2012. Depletion of intracellular zinc inhibits the ubiquitin ligase activity of the viral regulatory protein ICP0 and restricts herpes simplex virus 1 replication in cell culture. J. Virol. **86**:4029–4033. doi:10.1128/JVI.06962-11.
40. **Gu H, Roizman B.** 2003. The degradation of promyelocytic leukemia and Sp100 proteins by herpes simplex virus 1 is mediated by the ubiquitin-conjugating enzyme UbcH5a. Proc. Natl. Acad. Sci. U. S. A. **100**:8963–8968.
41. **Hagglund R, Roizman B.** 2002. Characterization of the novel E3 ubiquitin ligase encoded in exon 3 of herpes simplex virus-1-infected cell protein 0. Proc. Natl. Acad. Sci. U. S. A. **99**:7889–7894.
42. **Hagglund R, Van Sant C, Lopez P, Roizman B.** 2002. Herpes simplex virus 1-infected cell protein 0 contains two E3 ubiquitin ligase sites specific for different E2 ubiquitin-conjugating enzymes. Proc. Natl. Acad. Sci. U. S. A. **99**:631–636.
43. **Harris RA, Everett RD, Zhu XX, Silverstein S, Preston CM.** 1989. Herpes simplex virus type 1 immediate-early protein Vmw110 reactivates latent herpes simplex virus type 2 in an in vitro latency system. J. Virol. **63**:3513–3515.
44. **Kumar S, Nei M, Dudley J, Tamura K.** 2008. MEGA: a biologist-centric software for evolutionary analysis of DNA and protein sequences. Brief. Bioinform. **9**:299–306.
45. **Labute P.** 2008. The generalized Born/volume integral implicit solvent model: estimation of the free energy of hydration using London dispersion instead of atomic surface area. J. Comput. Chem. **29**:1693–1698.
46. **Lees-Miller SP, et al.** 1996. Attenuation of DNA-dependent protein kinase activity and its catalytic subunit by the herpes simplex virus type 1 transactivator ICP0. J. Virol. **70**:7471–7477.
47. **Leib DA, et al.** 1989. Immediate-early regulatory gene mutants define different stages in the establishment and reactivation of herpes simplex virus latency. J. Virol. **63**:759–768.
48. **Levitt M.** 1992. Accurate modeling of protein conformation by automatic segment matching. J. Mol. Biol. **226**:507–533.
49. **Lilley CE, et al.** 2010. A viral E3 ligase targets RNF8 and RNF168 to control histone ubiquitination and DNA damage responses. EMBO J. **29**:943–955.
50. **Lium EK, Silverstein S.** 1997. Mutational analysis of the herpes simplex virus type 1 ICP0 C_3HC_4 zinc ring finger reveals a requirement for ICP0 in the expression of the essential α27 gene. J. Virol. **71**:8602–8614.
51. **Lomonte P, Everett RD.** 1999. Herpes simplex virus type 1 immediate-early protein Vmw110 inhibits progression of cells through mitosis and from G_1 into S phase of the cell cycle. J. Virol. **73**:9456–9467.
52. **Lomonte P, Morency E.** 2007. Centromeric protein CENP-B proteasomal degradation induced by the viral protein ICP0. FEBS Lett. **581**:658–662.
53. **Lomonte P, Sullivan KF, Everett RD.** 2001. Degradation of nucleosome-associated centromeric histone H3-like protein CENP-A induced by herpes simplex virus type 1 protein ICP0. J. Biol. Chem. **276**:5829–5835.
54. **Lukashchuk V, Everett RD.** 2010. Regulation of ICP0-null mutant herpes simplex virus type 1 infection by ND10 components ATRX and hDaxx. J. Virol. **84**:4026–4040.
55. **Markson G, et al.** 2009. Analysis of the human E2 ubiquitin conjugating enzyme protein interaction network. Genome Res. **19**:1905–1911.
56. **Meredith M, Orr A, Elliott M, Everett R.** 1995. Separation of sequence requirements for HSV-1 Vmw110 multimerisation and interaction with a 135-kDa cellular protein. Virology **209**:174–187.
57. **Meredith M, Orr A, Everett R.** 1994. Herpes simplex virus type 1 immediate-early protein Vmw110 binds strongly and specifically to a 135-kDa cellular protein. Virology **200**:457–469.
58. **Morris JR, et al.** 2006. Genetic analysis of BRCA1 ubiquitin ligase activity and its relationship to breast cancer susceptibility. Hum. Mol. Genet. **15**:599–606.
59. **Müller S, Dejean A.** 1999. Viral immediate-early proteins abrogate the

modification by SUMO-1 of PML and Sp100 proteins, correlating with nuclear body disruption. J. Virol. **73**:5137–5143.
60. **O'Rourke D, Elliott G, Papworth M, Everett R, O'Hare P.** 1998. Examination of determinants for intranuclear localization and transactivation within the RING finger of herpes simplex virus type 1 IE110k protein. J. Gen. Virol. **79**(Pt 3):537–548.
61. **Parkinson J, Lees-Miller SP, Everett RD.** 1999. Herpes simplex virus type 1 immediate-early protein vmw110 induces the proteasome-dependent degradation of the catalytic subunit of DNA-dependent protein kinase. J. Virol. **73**:650–657.
62. **Preston CM, Mabbs R, Nicholl MJ.** 1997. Construction and characterization of herpes simplex virus type 1 mutants with conditional defects in immediate early gene expression. Virology **229**:228–239.
63. **Preston CM, Nicholl MJ.** 2005. Human cytomegalovirus tegument protein pp71 directs long-term gene expression from quiescent herpes simplex virus genomes. J. Virol. **79**:525–535.
64. **Preston CM, Nicholl MJ.** 1997. Repression of gene expression upon infection of cells with herpes simplex virus type 1 mutants impaired for immediate-early protein synthesis. J. Virol. **71**:7807–7813.
65. **Stow ND, Stow EC.** 1986. Isolation and characterization of a herpes simplex virus type 1 mutant containing a deletion within the gene encoding the immediate early polypeptide Vmw110. J. Gen. Virol. **67**(Pt 12): 2571–2585.
66. **Thompson RL, Preston CM, Sawtell NM.** 2009. De novo synthesis of VP16 coordinates the exit from HSV latency in vivo. PLoS Pathog. **5**:e1000352.
67. **Thompson RL, Sawtell NM.** 2006. Evidence that the herpes simplex virus type 1 ICP0 protein does not initiate reactivation from latency in vivo. J. Virol. **80**:10919–10930.
68. **Van Sant C, Hagglund R, Lopez P, Roizman B.** 2001. The infected cell protein 0 of herpes simplex virus 1 dynamically interacts with proteasomes, binds and activates the cdc34 E2 ubiquitin-conjugating enzyme, and possesses in vitro E3 ubiquitin ligase activity. Proc. Natl. Acad. Sci. U. S. A. **98**:8815–8820.
69. **van Wijk SJ, et al.** 2009. A comprehensive framework of E2-RING E3 interactions of the human ubiquitin-proteasome system. Mol. Syst. Biol. **5**:295.
70. **Wang J, Cieplak P, Kollman PA.** 2000. How well does a restrained electrostatic potential (RESP) model perform in calculating conformational energies of organic and biological molecules? J. Comput. Chem. **21**:1049–1074.
71. **Yao F, Schaffer PA.** 1995. An activity specified by the osteosarcoma line U2OS can substitute functionally for ICP0, a major regulatory protein of herpes simplex virus type 1. J. Virol. **69**:6249–6258.
72. **Zheng N, Wang P, Jeffrey PD, Pavletich NP.** 2000. Structure of a c-Cbl-UbcH7 complex: RING domain function in ubiquitin-protein ligases. Cell **102**:533–539.